

# Regulation of stability and function of the epithelial Na<sup>+</sup> channel (ENaC) by ubiquitination

O. Staub, I. Gautschi<sup>1</sup>, T. Ishikawa, K. Breitschopf<sup>2</sup>, A. Ciechanover<sup>2</sup>, L. Schild<sup>1</sup> and D. Rotin<sup>3</sup>

The Hospital for Sick Children, Division of Respiratory Research, 555 University Avenue, Toronto, Ontario M5G 1X8 and Biochemistry Department, University of Toronto, Toronto, Canada. <sup>1</sup>Institut de Pharmacologie et de Toxicologie, Université de Lausanne, CH-1015 Lausanne, Switzerland and <sup>2</sup>Biochemistry Department, Faculty of Medicine, Technion-Israel Institute of Technology, Haifa 31096, Israel

<sup>3</sup>Corresponding author  
e-mail: drotin@sickkids.on.ca

The epithelial Na<sup>+</sup> channel (ENaC), composed of three subunits ( $\alpha\beta\gamma$ ), plays a critical role in salt and fluid homeostasis. Abnormalities in channel opening and numbers have been linked to several genetic disorders, including cystic fibrosis, pseudohypoaldosteronism type I and Liddle syndrome. We have recently identified the ubiquitin-protein ligase Nedd4 as an interacting protein of ENaC. Here we show that ENaC is a short-lived protein ( $t_{1/2} \sim 1$  h) that is ubiquitinated *in vivo* on the  $\alpha$  and  $\gamma$  (but not  $\beta$ ) subunits. Mutation of a cluster of Lys residues (to Arg) at the N-terminus of  $\gamma$ ENaC leads to both inhibition of ubiquitination and increased channel activity, an effect augmented by N-terminal Lys to Arg mutations in  $\alpha$ ENaC, but not in  $\beta$ ENaC. This elevated channel activity is caused by an increase in the number of channels present at the plasma membrane; it represents increases in both cell-surface retention or recycling of ENaC and incorporation of new channels at the plasma membrane, as determined by Brefeldin A treatment. In addition, we find that the rapid turnover of the total pool of cellular ENaC is attenuated by inhibitors of both the proteasome and the lysosomal/endosomal degradation systems, and propose that whereas the unassembled subunits are degraded by the proteasome, the assembled  $\alpha\beta\gamma$ ENaC complex is targeted for lysosomal degradation. Our results suggest that ENaC function is regulated by ubiquitination, and propose a paradigm for ubiquitination-mediated regulation of ion channels.

**Keywords:** ENaC/half-life/lysosome/proteasome/ubiquitination

## Introduction

Amiloride-sensitive epithelial Na<sup>+</sup> channels, located at the apical membrane of Na<sup>+</sup>-transporting epithelia, play an essential role in the control of salt and fluid homeostasis in the kidney and the colon (Rossier and Palmer, 1992), as well as in fluid clearance from the alveolar space at birth and during pulmonary oedema (Saumon and Basset,

1993; O'Brodovich, 1995). These channels are tightly regulated by hormones such as aldosterone, vasopressin and insulin as well as PKA/cAMP, PKC, Ca<sup>2+</sup> and G proteins (Garty and Palmer, 1997).

The amiloride-sensitive epithelial Na<sup>+</sup> channel (ENaC) was cloned recently from rat (Canessa *et al.*, 1993, 1994a; Lingueglia *et al.*, 1993, 1994), human (McDonald *et al.*, 1994, 1995; Voilley *et al.*, 1994) and other species, and shown to be composed of three homologous subunits,  $\alpha$ -,  $\beta$ - and  $\gamma$ ENaC. Each subunit consists of two transmembrane regions, a large extracellular domain and cytosolic N- and C-termini (Canessa *et al.*, 1994b; Renard *et al.*, 1994; Snyder *et al.*, 1994) including proline-rich regions in each C-terminus (Rotin *et al.*, 1994; Staub *et al.*, 1996). Proper function of ENaC is crucial, as indicated by the finding that a gene knockout of  $\alpha$ ENaC is lethal due to the inability of the  $-/-$  mice to clear fluid from their lungs shortly after birth (Hummler *et al.*, 1996). Abnormally high ENaC activity has been also demonstrated in cystic fibrosis patients (Stutts *et al.*, 1995). Moreover, several inherited human disorders were recently linked by genetic linkage analysis to mutations in the ENaC subunits. These include the salt-wasting disease pseudohypoaldosteronism type 1 (PHA1, Chang *et al.*, 1996; Strautnieks *et al.*, 1996) and Liddle syndrome, an inherited autosomal dominant form of human hypertension (Liddle *et al.*, 1963; Botero-Velez *et al.*, 1994). In all these disorders, alteration in channel gating and/or numbers has been associated with the disease (Chang *et al.*, 1996; Firsov *et al.*, 1996).

We have recently identified the ubiquitin-protein ligase Nedd4 as an interacting protein of ENaC (Staub *et al.*, 1996), and therefore wanted to investigate whether ENaC is ubiquitinated in living cells and whether such putative ubiquitination is involved in regulating channel number and function. Ubiquitination of cellular proteins usually serves to tag them for rapid degradation (reviewed in Ciechanover, 1994; Jentsch and Schlenker, 1995). It involves the covalent attachment of ubiquitin or a poly-ubiquitin tree onto lysine residues in target proteins. Several enzymes are involved in this process, including a ubiquitin-activating enzyme (E1), a ubiquitin-conjugating enzyme (E2) and a ubiquitin-protein ligase (E3). In most studies described to date, ubiquitinated proteins are degraded by the 26S proteasome, a cytosolic threonine protease complex (Jentsch and Schlenker, 1995; Hilt and Wolf, 1996). Extensive work has implicated the involvement of the ubiquitin-proteasome system in regulating/degrading numerous cytosolic proteins, including several cell cycle proteins (e.g. cyclin A, B, C1b5p, cln 1, 2, 3p, SIC1) (reviewed in Deshaies, 1995), NF $\kappa$ B and I $\kappa$ B (Palombella *et al.*, 1994), and the nuclear proteins c-Jun (Treier *et al.*, 1994) and p53 (Scheffner *et al.*, 1993). In addition, recent evidence suggests that ER-associated protein degradation of either misfolded or improperly

assembled protein complexes involves the proteasome in either a ubiquitin-dependent or -independent fashion (reviewed in Brodsky and McCracken, 1997). For example, the immature form of CFTR becomes ubiquitinated in the ER and degraded by the proteasome (Jensen *et al.*, 1995; Ward *et al.*, 1995).

In recent years, it has become apparent that some transmembrane proteins also become ubiquitinated, and that ubiquitination is involved in their subsequent degradation by the endosomal/lysosomal pathway (reviewed in Hochstrasser, 1996). Examples of mammalian transmembrane proteins which become ubiquitinated include several tyrosine kinase receptors (e.g. EGFR, PDGFR, c-kit), cytokine receptors (e.g. T cell and IgE receptors) (Cenciarelli *et al.*, 1992; Mori *et al.*, 1992; Paolini and Kinet, 1993; Miyazawa *et al.*, 1994; Galcheva-Garbova *et al.*, 1995) and the growth hormone receptor, in which ligand-induced, ubiquitination-dependent endosomal/lysosomal degradation of the receptor was recently demonstrated (Strous *et al.*, 1996). In yeast, the membrane receptor Ste2 (Hicke and Riezman, 1996) and membrane transporters Ste6 and Pdr5 (Kölling and Hollenberg, 1994; Egner and Kuchler, 1996), as well as several yeast amino acid permeases including Gap1 and Fur4 (Hein *et al.*, 1995; Galan *et al.*, 1996), have been shown to become ubiquitinated, a necessary step for their subsequent degradation in the vacuoles. The exact degradation pathway for ubiquitinated transmembrane proteins, and the possible involvement of the proteasome complex in this process, is not known (Hochstrasser, 1996).

In this report we show that ENaC is a short-lived protein which becomes ubiquitinated in living cells on the  $\alpha$  and  $\gamma$  subunits. The rapid turnover of ENaC is sensitive to inhibitors of both the lysosomal and proteasomal degradation systems; whereas excess of unassembled (or misfolded) subunits are degraded by the proteasome, our data suggest that the assembled  $\alpha\beta\gamma$ ENaC complex is targeted to the lysosome. Moreover, mutating a cluster of lysines (to arginines) at the N-terminus of  $\gamma$ ENaC, or  $\alpha$ - plus  $\gamma$ ENaC, causes reduced ubiquitination, slower turnover and increased  $\text{Na}^+$  channel activity due to increased number of channels at the plasma membrane. Using Brefeldin A treatment, we demonstrate that this increase is caused by an elevated number of mutant channels retained at the cell surface, as well as by increased incorporation of mutant channels into the plasma membrane. These results suggest that ubiquitination of ENaC controls the number of channels at the plasma membrane, and provides a powerful means to regulate channel function.

## Results

### ENaC subunits are short-lived proteins with a rapid turnover rate

We have shown previously (Staub *et al.*, 1996) that the ubiquitin protein ligase Nedd4 binds to ENaC. Since ubiquitination of proteins is usually associated with their rapid turnover, we initially investigated the turnover rate of  $\alpha\beta\gamma$ ENaC using pulse-chase experiments. For these and all subsequent experiments, we used rat  $\alpha\beta\gamma$ ENaC (rENaC), which share ~85% overall amino acid sequence identity with the corresponding human ENaC (hENaC)

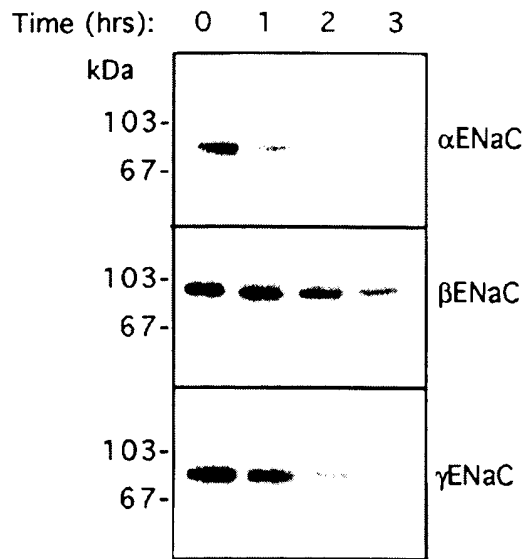


**Fig. 1.** Half-life of  $\alpha\beta\gamma$ ENaC. Pulse-chase experiments of  $^{35}\text{S}$ -labelled  $\alpha$  (upper panel),  $\beta$  (middle panel) and  $\gamma$  (lower panel) rat ENaC (called ENaC) stably expressed together in epithelial MDCK cells. Cells were labelled with [ $^{35}\text{S}$ ]Met and Cys for 2 h and chased for the indicated times (hrs). The calculated  $t_{1/2}$  values are:  $\alpha$ ENaC:  $1.13 \pm 0.13$  (mean  $\pm$  SE,  $n = 9$ ) h;  $\gamma$ ENaC:  $1.23 \pm 0.09$  (mean  $\pm$  SE,  $n = 6$ ) h;  $\beta$ ENaC:  $t_{1/2} > 3$  h. Similar results were obtained with NIH-3T3 cells (not shown).

subunits (Canessa *et al.*, 1993, 1994a; McDonald *et al.*, 1994, 1995). Pulse-chase experiments were performed with either kidney epithelial MDCK cells or with NIH-3T3 fibroblasts previously triple-transfected and stably expressing  $\alpha\beta\gamma$ ENaC (Stutts *et al.*, 1995). Cells were labelled for 2 h with [ $^{35}\text{S}$ ]methionine/cysteine and then chased for various periods of time. The  $\alpha\beta\gamma$ ENaC proteins were subsequently immunoprecipitated with antibodies directed against each of the ENaC subunits, and separated on SDS-PAGE (Figure 1). Following SDS-PAGE and autoradiography, bands were excised and radioactivity quantified by scintillation counting to determine half-life ( $t_{1/2}$ ) of the proteins. As is evident from Figure 1A,  $\alpha$ - and  $\gamma$ ENaC expressed in MDCK cells have a rapid turnover rate with a half-life of ~1 h;  $\beta$ ENaC, on the other hand, has a longer half-life ( $t_{1/2} > 3$  h). The half-life of the ENaC subunits measured following 1 h pulse was the same as that following 2 h pulse (not shown). In addition, the turnover rates of  $\alpha\beta\gamma$ ENaC expressed in NIH-3T3 cells were very similar to those expressed in MDCK cells (data not shown).

### $\alpha$ - and $\gamma$ ENaC, but not $\beta$ ENaC, are ubiquitinated in vivo

A rapid turnover of proteins is often associated with ubiquitination-mediated degradation. We thus wanted to test whether the  $\alpha\beta\gamma$ ENaC subunits are ubiquitinated in living cells. For these experiments, we used epitope-tagged  $\alpha$ - or  $\gamma$ ENaC because the antibodies available against these native subunits, unlike the antibodies against native  $\beta$ ENaC, are not sensitive enough for immunoblotting. We subcloned HA-tagged  $\alpha$ ENaC, FLAG-tagged  $\gamma$ ENaC or untagged  $\beta$ ENaC into CMV-based expression vectors. The HA or FLAG tags were added just upstream

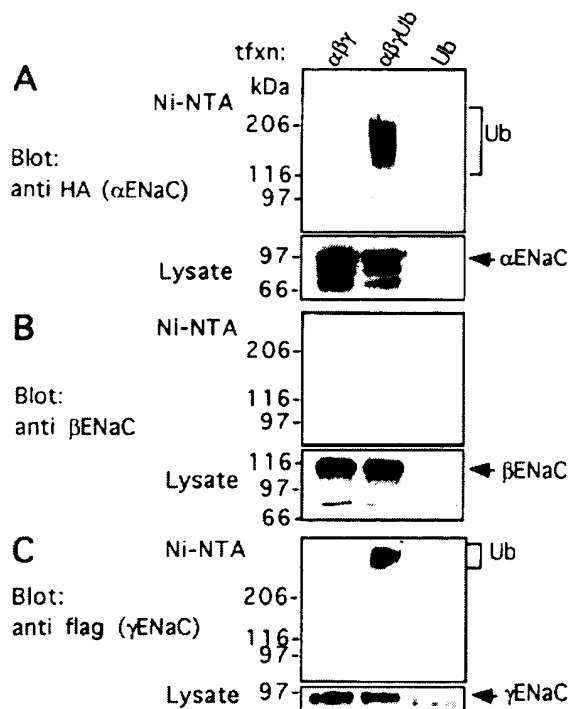


**Fig. 2.** Ubiquitination of  $\alpha$  and  $\gamma$ , but not  $\beta$ , ENaC expressed in Hek-293 cells. Hek-293 cells transiently co-transfected (tfxn) with HA-tagged  $\alpha$ ENaC ( $\alpha$ ), FLAG-tagged  $\gamma$ ENaC ( $\gamma$ ),  $\beta$ ENaC ( $\beta$ ) and/or the His-Ub (Ub) construct were lysed and lysates incubated with  $\text{Ni}^{2+}$ -NTA agarose beads ( $\text{Ni}^{2+}$ -NTA) to precipitate histidinated (ubiquitinated) proteins. These proteins were separated on 7% SDS-PAGE, transferred to nitrocellulose and blotted with (A) anti-HA antibodies (to detect ubiquitinated  $\alpha$ ENaC), (B) anti- $\beta$ ENaC antibodies (to detect ubiquitinated  $\beta$ ENaC) and (C) anti-FLAG (flag) antibodies (to detect ubiquitinated  $\gamma$ ENaC). Ubiquitinated species appear as a cluster of high molecular weight bands (upper panels, square brackets). Lower panels of each blot (Lysate) represent expression of the transfected protein ( $\alpha$ -,  $\beta$ - or  $\gamma$ ENaC) in the lysates. Arrows indicate fully glycosylated forms of ENaC subunits.

of the stop codons of  $\alpha$ - or  $\gamma$ ENaC respectively, since tagging at these sites had no effect on channel activity (not shown). We then transiently co-transfected HA-tagged  $\alpha$ ENaC, FLAG-tagged  $\gamma$ ENaC and  $\beta$ ENaC together with a plasmid encoding His-tagged multiubiquitin (His-Ub) (Treier *et al.*, 1994) (kindly provided by D. Bohmann) into Hek-293 cells. These cells were chosen because MDCK cells are not easily amenable to transient transfections. The  $\alpha\beta\gamma$ ENaC subunits were expressed together (in Hek-293 cells) to allow for the formation of a functional channel complex that is able to reach the plasma membrane (Canessa *et al.*, 1994a; Firsov *et al.*, 1996). Twenty-four hours after transfection, cells were lysed, denatured with 2% SDS, diluted with lysis buffer and the diluted lysates incubated with  $\text{Ni}^{2+}$ -NTA beads to allow for binding of the histidinated (and therefore ubiquitinated) proteins. After thorough washes, bound proteins were eluted and separated on SDS-PAGE, followed by immunoblotting with either anti-HA (i.e. anti- $\alpha$ ENaC), anti-FLAG (i.e. anti- $\gamma$ ENaC), or anti- $\beta$ ENaC antibodies directed against the C-terminus of  $\beta$ ENaC (kindly provided by B.C. Rossier). As can be seen in Figure 2A, B and C (bottom panels, lysates),  $\alpha$ -,  $\beta$ - and  $\gamma$ ENaC were all expressed

in the transfected cells (in the same experiment). The precipitation of His-tagged (ubiquitinated) proteins from lysates of these transfected cells (with  $\text{Ni}^{2+}$ -NTA beads) revealed high molecular weight ubiquitinated species of  $\alpha$ ENaC (Figure 2A, top panel, bracket) and  $\gamma$ ENaC (Figure 2C, top panel, bracket), as detected by anti-HA or anti-FLAG antibodies respectively; these ubiquitinated ENaC proteins were only detected in cells co-transfected with the His-Ub construct, and not in cells transfected with the ENaC subunits alone or with the His-Ub construct alone (Figure 2A, B and C, top panels). In contrast to  $\alpha$ - or  $\gamma$ ENaC, the  $\beta$ ENaC subunit was not ubiquitinated (Figure 2B, upper panel), even though  $\beta$ ENaC was strongly expressed in these cells (Figure 2B, lower panel). The ubiquitination of  $\alpha$ - and  $\gamma$ ENaC did not seem to be a peculiar property of one cell line, because it was also observed in transfected COS-7 cells (not shown). These results, therefore, demonstrate that in  $\alpha\beta\gamma$ ENaC-transfected cells,  $\alpha$  and  $\gamma$ ENaC, but not  $\beta$ ENaC, are ubiquitinated *in vivo*.

#### Mutation of conserved N-terminal lysines hyperactivates ENaC channel activity

Ubiquitination of proteins is mediated by the addition of ubiquitin or multiubiquitin groups onto Lys residues. Since we identified ubiquitination of  $\alpha$ - and  $\gamma$ ENaC *in vivo*, we wanted to investigate whether mutation of Lys residues, which may serve as the ubiquitin attachment sites, could lead to increased  $\text{Na}^+$  channel activity. Inspection of the sequences of rat (r) and human (h)  $\alpha\beta\gamma$ ENaC (Canessa *et al.*, 1994a; McDonald *et al.*, 1994, 1995) revealed conserved Lys residues at the N-termini of these subunits (Figure 3). Most of these lysines are also conserved in xENaC, the *Xenopus* homologue of ENaC (Puoti *et al.*, 1995). The cytosolic C-termini of these subunits are largely devoid of lysines, and the one or two lysines that are present in  $\beta$ - or  $\gamma$ ENaC (respectively) are very close to the transmembrane domain and are not conserved. We therefore mutated the conserved lysines at the N-termini of  $\alpha$ -,  $\beta$ - and  $\gamma$ ENaC (herein referred to as  $\alpha\beta\gamma$ ENaC) to arginines either individually or in groups in those cases where the lysines were clustered close to each other. The mutants generated were as follows (see Figure 3): (i) In  $\alpha$ ENaC: K47 and K50 ( $\alpha$ K47,50R), K108 ( $\alpha$ K108R) or  $\alpha$ K47,50R plus  $\alpha$ K108R ( $\alpha$ K47,50,108R). An additional  $\alpha$ ENaC construct was also generated, in which lysines 23, 26 and 32 (which are not conserved between rat and human) of the  $\alpha$ K47,50R construct were mutated to Arg, yielding the mutant  $\alpha$ K23-50R. (ii) In  $\beta$ ENaC: K4, K5 and K9 ( $\beta$ K4,5,9R) or K16, K23, K39, K47, K48 and K49 ( $\beta$ K16-49R). (iii) In  $\gamma$ ENaC: K6, K8, K10, K12, K13 ( $\gamma$ K6-13R), K26R ( $\gamma$ K26R) or K6-13 plus K26R ( $\gamma$ K6-13+26R).

We then investigated the effect of the above Lys to Arg mutations in  $\alpha\beta\gamma$ ENaC on ENaC channel activity. Two-electrode voltage clamp experiments were performed in which amiloride-sensitive  $\text{Na}^+$  currents ( $I_{\text{Na}}$ ) were measured in *Xenopus* oocytes expressing the different Lys to Arg mutants. Our results show that none of the conserved Lys to Arg  $\alpha$ ENaC mutants, when expressed together with wild type (wt)  $\beta\gamma$ ENaC, had any effect on increasing ENaC activity (Figure 4A). This lack of effect on ENaC function was also observed with the extended  $\alpha$ K23-50R

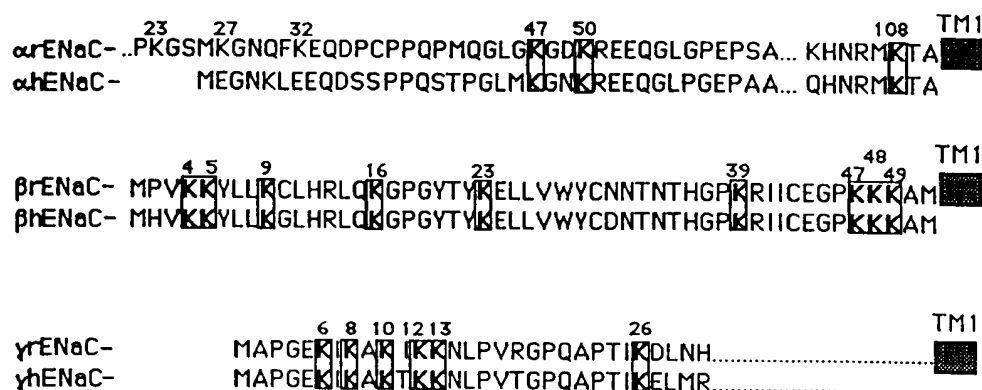


Fig. 3. N-terminal Lys to Arg mutants of  $\alpha\beta\gamma$ ENaC. Schematic representation of the conserved lysine residues at the N-termini of  $\alpha\beta\gamma$ ENaC and  $\alpha\beta\gamma$ hENaC. All conserved lysines (Bold letters, boxed), as well as three non-conserved lysine residues in  $\alpha$ ENaC, are numbered according to the published rat ENaC sequences (Canessa *et al.*, 1994a). The numbered lysines were mutated to arginines to create the following mutant constructs: in  $\alpha$ ENaC:  $\alpha$ K47,50R,  $\alpha$ K108R,  $\alpha$ K47,50,108R and  $\alpha$ K23-50R; in  $\beta$ ENaC:  $\beta$ K4,5,9R and  $\beta$ K16-49R; in  $\gamma$ ENaC:  $\gamma$ K6-13R,  $\gamma$ K26R and  $\gamma$ K6-13R + K26R. (TM1 = the first transmembrane domain of each ENaC subunit.)

mutant (not shown). Similarly, none of the Lys to Arg mutations within the N-terminus of  $\beta$ ENaC, expressed together with wt- $\alpha\gamma$ ENaC, caused any increase in amiloride-sensitive  $\text{Na}^+$  currents. In contrast, the expression of the  $\gamma$ ENaC mutants ( $\gamma$ K6-13R or  $\gamma$ K6-13+26R) together with wt- $\alpha\beta$ ENaC more than doubled  $\text{Na}^+$  channel activity (Figure 4A). Moreover, when this  $\gamma$ K6-13R mutant was co-expressed together with the  $\alpha$ K47,50R mutant (along with wt- $\beta$ ENaC), the hyperactivation of ENaC was potentiated, yielding up to 6-fold stimulation of  $\text{Na}^+$  channel activity when compared to the activity of the wt channel (Figure 4A). In contrast, such potentiation was not observed when the  $\beta$ K4,5,9R or the  $\beta$ K16-49R mutant was co-expressed with either  $\alpha$ K47,50R,  $\gamma$ K6-13R or both mutants (Figure 4A). These results therefore demonstrate that a cluster of conserved Lys residues particularly in  $\gamma$ ENaC, but also in  $\alpha$ ENaC, are responsible for the regulation of ENaC activity, and when mutated, lead to an increase in amiloride sensitive  $\text{Na}^+$  current ( $I_{\text{Na}}$ ). Moreover our data show that the Lys to Arg substitutions increase channel activity only when performed on subunits previously shown to be ubiquitinated *in vivo* ( $\alpha$ - and  $\gamma$ ENaC).

#### Lys to Arg mutations in $\gamma$ ENaC, or in $\alpha$ - plus $\gamma$ ENaC, lead to an increase of $\text{Na}^+$ channel numbers at the cell surface

The elevated  $\text{Na}^+$  channel activity associated with the Lys to Arg mutations in  $\gamma$ ENaC or  $\alpha$ - plus  $\gamma$ ENaC was determined by an increase in amiloride-sensitive  $\text{Na}^+$  current. In theory, such an increase can result from either an increase in the number of channels (N) expressed at the cell surface, and/or higher  $\text{Na}^+$  influx per channel molecule when the open probability ( $P_o$ ) or single channel conductance are increased. Analysis by patch clamp technique of single channel currents of the  $\alpha$ K47,50R plus  $\gamma$ K6-13R double mutant (Figure 4B) revealed a high number of active channels per patch without significant changes in single channel conductance for  $\text{Li}^+$  ions, a highly permeant cation in ENaC. The conductance for  $\text{Li}^+$  ions of 8–9 pS was similar to that found for wt-ENaC (Schild *et al.*, 1997), indicating that these Lys to Arg

mutations did not affect the conductive properties of the channel. To distinguish between changes in the channel open probability and increased surface expression of ENaC, we used a quantitative binding assay to correlate in individual oocytes the amiloride-sensitive  $I_{\text{Na}}$  with the number of channel molecules present at the cell surface, as previously described (Firsov *et al.*, 1996). This binding assay uses specific  $^{125}\text{I}$ -labelled antibodies directed against a FLAG epitope introduced into the extracellular domain of each of the  $\alpha\beta\gamma$ ENaC subunits (wt or the above Lys to Arg mutants), as described in Materials and methods. Such epitope tagging does not interfere with channel function (Firsov *et al.*, 1996). Figure 6A and B show representative experiments in which amiloride-sensitive  $I_{\text{Na}}$  and surface expression of wt-ENaC or Lys to Arg mutants of  $\alpha$ - and  $\gamma$ ENaC ( $\alpha$ K47,50R;  $\gamma$ K6-13R;  $\alpha$ K47,50R +  $\gamma$ K6-13R) were measured in individual oocytes. The Lys to Arg mutants of  $\beta$ ENaC were not tested since none of them was able to elevate channel activity (Figure 4A). Comparing the ENaC mutants with wt confirms that the  $\alpha$ K47,50R mutations did not increase the amiloride sensitive  $\text{Na}^+$  current (as shown in Figure 4A) or the number of channel molecules expressed at the cell surface (Figure 5A). For the  $\gamma$ K6-13R or the  $\alpha$ K47,50R plus  $\gamma$ K6-13R double mutant, the increase in  $I_{\text{Na}}$  relative to wt-ENaC was directly proportional to the increase in the number of binding sites recognized by the anti-FLAG antibodies. The significant linear correlation between the current expressed and the number of ENaC channel molecules indicates that the  $\text{Na}^+$  current per channel was not significantly altered in the Lys to Arg mutants relative to wt-ENaC. These results are summarized quantitatively in Figure 5C. Since the  $I_{\text{Na}}$  measured in the Lys to Arg mutants increased linearly with the specific binding of the anti-FLAG antibodies, we conclude that this increase was caused by an elevated number of channels at the cell surface, and not by changes in the channel open probability. This increase in number of channels at the plasma membrane induced by the Lys to Arg mutations in the  $\alpha$  and  $\gamma$  subunits would be consistent with an inhibition of ubiquitination of the channel protein.

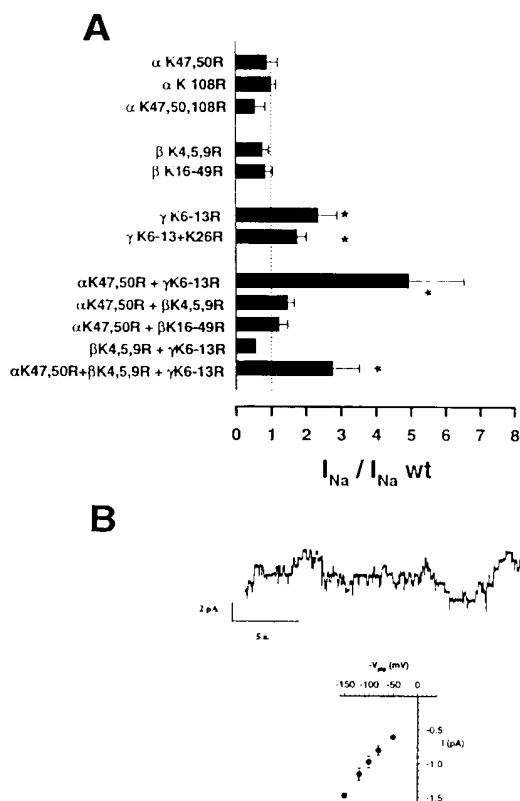


**Fig. 4.**  $Na^+$  channel activity of Lys to Arg mutants of  $\alpha\beta\gamma$ ENaC expressed in *Xenopus* oocytes. (A) cRNA derived from the Lys to Arg mutants of  $\alpha$ -,  $\beta$ - or  $\gamma$ ENaC (depicted in Figure 3) was injected individually or in combination into oocytes, together with wild type (wt) ENaC cRNA of the remaining ENaC subunits and amiloride-sensitive  $Na^+$  currents ( $I_{Na}$ ) measured by the two electrode voltage clamp technique. Bars represent means  $\pm$  SE of four independent experiments each with 8–10 oocytes. Asterisks denote statistically significant differences ( $P < 0.05$ ) from wt-ENaC. (B) Upper panel: Representative single channel recording of the  $\alpha K47,50R + \gamma K6-13R$  (plus wt- $\beta$ ) ENaC double mutant in *Xenopus* oocytes using the patch-clamp technique in a cell-attached configuration, with  $Li^+$  ions as the major permeant ion in the patch pipet. Recording was performed at pipette potential ( $V_{pip}$ ) of 100 V. At least six active channels are present in the patch as shown by the different current levels, and downward deflexions represent channel openings. Lower panel: Current-voltage ( $I/V$ ) relationship of single channel  $Li^+$  currents measured between  $-50$  and  $-150$  mV and determined from five different channel recordings. Regression analysis of data points gives a single channel conductance for  $Li^+$  ions of 8.6 pS. Dotted line represents a fit to the constant field equation.

#### Inhibition of ubiquitination of the Lys to Arg mutants of $\gamma$ ENaC, or of $\alpha$ -plus $\gamma$ ENaC

As we observed an increase in channel activity resulting from a greater number of  $\alpha\beta\gamma$ ENaC at the plasma membrane in the  $\gamma K6-13R$  mutant, we wanted to test whether such increased cell surface number in ENaC channels is caused by impaired ubiquitination of this mutant. Since direct determination of ENaC ubiquitination in oocytes is not currently feasible due to limits of protein detection (since only a few oocytes can be analysed at a time, not sufficient for biochemical assays), we opted instead to use mammalian cells, which allow the use of a large number of cells per assay and are thus more suitable for biochemical studies. We therefore co-transfected Hek-293 cells with

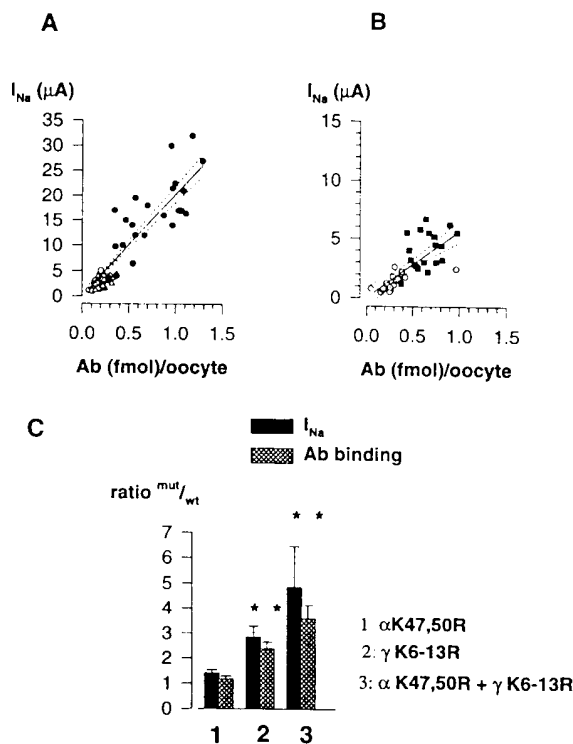


**Fig. 5.** Correlation of surface labelling and function of Lys to Arg mutants of  $\alpha$ - and  $\gamma$ ENaC measured in individual oocytes. (A and B) Representative experiments in which amiloride-sensitive  $I_{Na}$  and surface expression of wt-ENaC, or the indicated Lys to Arg mutants, were measured in individual oocytes. Surface expression was quantified by binding of anti-FLAG  $^{125}I$ -labelled antibody (Ab) to the FLAG-tagged ectodomains of (A) wt-ENaC (open circles),  $\alpha K47,50R$  (open triangles) or the  $\alpha K47,50R + \gamma K6-13R$  mutants (closed circles), and (B) wt-ENaC (open circles) or the  $\gamma K6-13R$  mutant (closed squares). Solid lines represent regression analysis of the data. Dotted lines represent the 95% confidence limits. (C) Summary histogram showing changes of the amiloride-sensitive current ( $I_{Na}$ ) and specific cell surface binding of Ab, relative to the values obtained with wt-ENaC. Values are mean  $\pm$  SE of four to five independent experiments in which average  $I_{Na}$  and antibody binding were determined from simultaneous measurements in eight to ten individual oocytes. Asterisks denote statistical significance at  $P < 0.05$  level.

the His-Ub construct together with either wt- $\alpha\beta\gamma$ ENaC (control), or wt- $\alpha\beta$ ENaC plus the  $\gamma K6-13R$  mutants of  $\gamma$ ENaC. As before, the  $\alpha$ ENaC constructs were HA-tagged and the  $\gamma$ ENaC constructs were FLAG-tagged. Following transfection, cells were lysed, and lysates incubated with  $Ni^{2+}$ -NTA beads to precipitate ubiquitinated proteins. These proteins were then separated on SDS-PAGE, transferred to nitrocellulose and immunoblotted with anti-FLAG antibodies, to detect the extent of ubiquitination of  $\gamma$ ENaC. Our results show that ubiquitination of  $\gamma$ ENaC was indeed inhibited in the  $\gamma K6-13R$  mutant (Figure 6A, upper panel, compare lanes 3 and 4), despite similar expression levels of the wt or mutant  $\gamma$ ENaC proteins in the lysate of the transfected cells (Figure 6A, lower panel, lanes 3 and 4). The same inhibition of ubiquitination of  $\gamma$ ENaC was also observed when the  $\gamma K6-13R$  mutant was expressed together with the  $\alpha K23-50R$  mutant of  $\alpha$ ENaC (Figure 6A, lanes 5 and 6). These results therefore demonstrate that those conserved Lys residues located at the N-terminus of  $\gamma$ ENaC which are involved in regulating

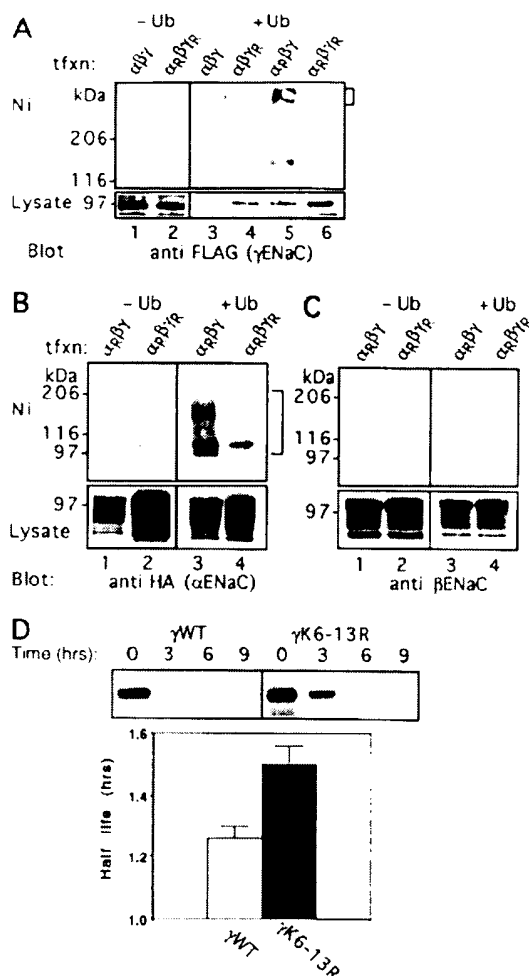


**Fig. 6.** Inhibition of ubiquitination of the Lys to Arg mutants of  $\gamma$ - and  $\alpha$ ENaC. Hek-293 cells were transiently co-transfected (tfxn) with  $\beta$ ENaC ( $\beta$ ), HA-tagged  $\alpha$ ENaC ( $\alpha$ ) or  $\alpha$ K23-50R ( $\alpha$ R), and FLAG-tagged  $\gamma$ ENaC ( $\gamma$ ) or  $\gamma$ K6-13R ( $\gamma$ R), with or without His-Ub (Ub). Cells were then lysed, and lysates incubated with  $\text{Ni}^{2+}$ -NTA agarose beads to precipitate ubiquitinated proteins. Precipitated proteins were separated on 7% SDS-PAGE, transferred to nitrocellulose and blotted with either (A) anti-FLAG ( $\gamma$ ENaC), (B) anti-HA ( $\alpha$ ENaC) or (C) anti- $\beta$ ENaC antibodies (upper panels), to detect ubiquitination of each subunit or its Lys to Arg mutants in the same experiment. Lower panels represent levels of expression of the transfected proteins in the lysate. Square brackets mark the ubiquitinated species of  $\alpha$  and  $\gamma$  ENaC. The ~105 kDa band across panel B (top) is probably a contaminant. (D)  $\gamma$ K6-13R mutant is more stable than wt- $\gamma$ ENaC. MDCK cells stably expressing wt- $\alpha\beta\gamma$ ENaC (called  $\gamma$ WT) or  $\gamma$ K6-13R plus wt- $\alpha\beta$ ENaC (called  $\gamma$ K6-13R) (both  $\gamma$  subunits FLAG-tagged at the C terminus, as in Figure 2 above) were labelled with [ $^{35}\text{S}$ ]Met-Cys and chased for the indicated times (hrs). Cells were then lysed, immunoprecipitated with anti  $\gamma$ ENaC antibodies, the immunoprecipitates separated on 7% SDS PAGE and visualized by autoradiography, as represented by the autoradiogram. Histogram represents  $t_{1/2}$  quantitation (mean  $\pm$  SE) of three independent experiments similar to that depicted in the autoradiogram.

channel stability at the plasma membrane ( $\gamma$ K6-13) indeed serve as attachment sites for ubiquitin.

We next wanted to determine the extent of ubiquitination of the Lys to Arg mutants of  $\alpha$ ENaC when expressed either with wt- $\beta\gamma$ ENaC or with the  $\gamma$ K6-13R mutant of  $\gamma$ ENaC (plus wt- $\beta$ ENaC). This was done in order to test

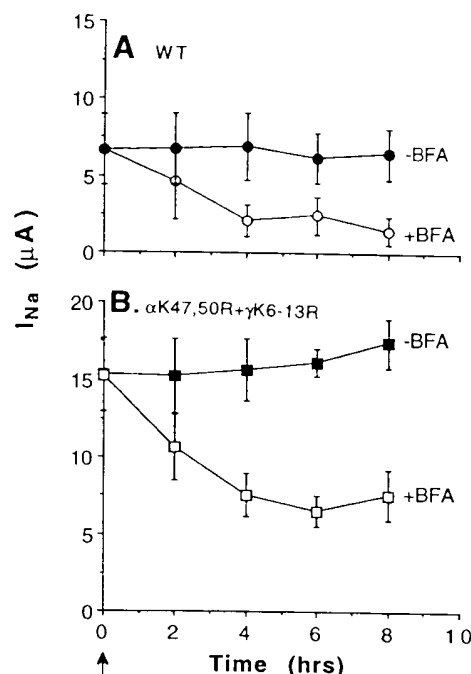


**Fig. 7.** The effect of Brefeldin A on channel activity of wt-ENaC or the  $\alpha$ K47,50R+ $\gamma$ K6-13R mutant. cRNA from (A) wt- $\alpha\beta\gamma$ ENaC (WT) or (B) the  $\alpha$ K47,50R+ $\gamma$ K6-13R (plus wt- $\beta$ ) mutant, was injected into *Xenopus* oocytes. Eighteen hours later, 10  $\mu\text{g/ml}$  Brefeldin A (BFA) were added (at time 0, arrow) to the bathing medium and amiloride-sensitive  $\text{Na}^+$  currents ( $I_{\text{Na}}$ ) measured by the two-electrode voltage clamp technique at the indicated times. Data points represent mean  $\pm$  SE of four separate experiments each performed with five oocytes.

whether the potentiation of ENaC hyperactivation and retention at the cell surface observed in the double mutant (i.e. Lys to Arg mutations in both  $\alpha$ - and  $\gamma$ ENaC) is associated with reduced ubiquitination of not only  $\gamma$ ENaC, but also of  $\alpha$ ENaC. We therefore re-probed the blot shown in Figure 6A with HA antibodies, to determine the extent of ubiquitination of  $\alpha$ ENaC in the same experiment. Our results show that the  $\alpha$ K23-50R mutant [similar to the  $\alpha$ K47,50R mutant (data not shown)] was still ubiquitinated when co-expressed with wt- $\beta\gamma$ ENaC and His-Ub (Figure 6B, lane 3). In contrast, however, there was a clear and reproducible inhibition of this ubiquitination when the  $\alpha$ K23-50R mutant was co-transfected with the  $\gamma$ K6-13R mutant (and wt- $\beta$ ENaC plus His-Ub) (Figure 6B, lane 4). This reduction in ubiquitination was apparent despite similar expression levels of the wt or mutant  $\alpha$ ENaC proteins (Figure 6B, lower panel). Thus, the combined removal of lysines 6–13 from  $\gamma$ ENaC together with N-terminal lysines from  $\alpha$ ENaC caused a reduction of ubiquitination of both subunits, in agreement with the observed potentiation of cell surface retention and activity of ENaC under these conditions. None of the above Lys to Arg mutations in  $\alpha$  or  $\gamma$ ENaC, or both, caused any detectable ubiquitination of  $\beta$ ENaC (Figure 7C).

Our data show that ENaC turnover is regulated by ubiquitination, and that removal of potential ubiquitination sites on  $\gamma$ ENaC ( $\gamma$ K6-13R) leads to stabilization of ENaC at the plasma membrane. A prediction of these data is that the half-life of the  $\gamma$ K6-13R mutant should be pro-

longed. We therefore generated stable MDCK cell lines which express either FLAG-tagged wt- $\gamma$  (control), or FLAG-tagged  $\gamma$ K6-13R mutant, together with wt- $\alpha$ ENaC (the FLAG tag does interfere with channel function, data not shown). We then performed a pulse-chase experiment as described in Figure 1 above. Our results show that  $\gamma$ ENaC bearing the K6-13R mutations was indeed more stable (mean  $t_{1/2} = 90$  min) than the wt- $\gamma$ ENaC (mean  $t_{1/2} = 76$  min), showing a small but statistically significant different ( $P = 0.027$ ) increase in half-life of the protein (Figure 6D).

Collectively, these results show that ENaC stability and activity is regulated by ubiquitination. The primary target for this ubiquitination-mediated regulation is a cluster of lysine residues (K6-13) at the N-terminus of  $\gamma$ ENaC, since mutation of these lysine residues was sufficient to both increase channel number at the plasma membrane and to reduce its ubiquitination.  $\alpha$ ENaC, but not  $\beta$ ENaC, is also playing a role in this regulation of channel stability by ubiquitination.

#### Accumulation of Brefeldin A-resistant pool of the Lys to Arg ENaC mutant at the cell surface

To test whether the impaired ubiquitination and increased channel number and activity of the Lys to Arg ENaC mutants is associated with increased arrival of newly synthesized channels at the plasma membrane, decreased degradation of cell surface-associated channels, or both, we tested the effect of Brefeldin A (BFA) on ENaC activity in *Xenopus* oocytes. Brefeldin A inhibits the ER to Golgi transport of newly synthesized membrane proteins, and has been previously shown to be effective in *Xenopus* oocytes (Geering *et al.*, 1996). Thus, cRNA of wt- $\alpha\beta\gamma$ ENaC (wt) or  $\alpha$ K47,50R+ $\gamma$ K6-13R (with wt- $\beta$ ) ENaC was injected into *Xenopus* oocytes and following overnight incubation, oocytes were treated with 10  $\mu$ g/ml BFA at time 0 (arrow) for up to 8 h, and amiloride-sensitive  $I_{Na}$ , representing active channels at the cell surface, measured by the two-electrode voltage clamp technique. Our results show that whereas the majority (~80%) of wt ENaC activity disappeared by 8 h exposure to BFA, 43% ( $\pm 7\%$ ) of the  $\alpha$ K47,50R+ $\gamma$ K6-13R mutant channel activity was BFA-resistant (Figure 7). The accumulation of this BFA-resistant pool was apparent after 4 h incubation, and suggests that a significant fraction of the  $\alpha$ K47,50R+ $\gamma$ K6-13R mutant, unlike the wt ENaC, is retained at the cell surface or is recycled between endocytic vesicles and the plasma membrane. However, the amount of BFA-sensitive pool at 8 h incubation was also greater in the  $\alpha$ K47,50R+ $\gamma$ K6-13R mutant than in the wt channel (average of 9.9  $\mu$ A versus 5  $\mu$ A respectively), suggesting that the rate of arrival of newly synthesized channels to the plasma membrane is also elevated in the Lys to Arg mutant. Thus, loss of ubiquitination sites in ENaC likely leads to both an increase in incorporation and increased retention/recycling of the channel at the plasma membrane.

#### ENaC degradation is sensitive to endosomal/lysosomal and to proteasome inhibitors

Degradation of ubiquitinated proteins is carried out either by the proteasomes (usually of cytosolic or misfolded, misassembled proteins in the ER) or by the endosomal-

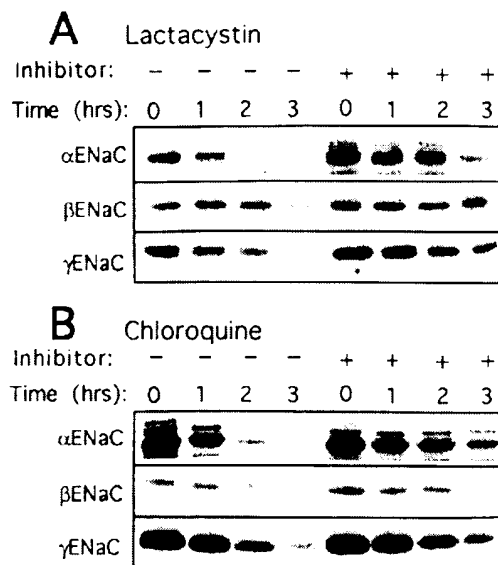
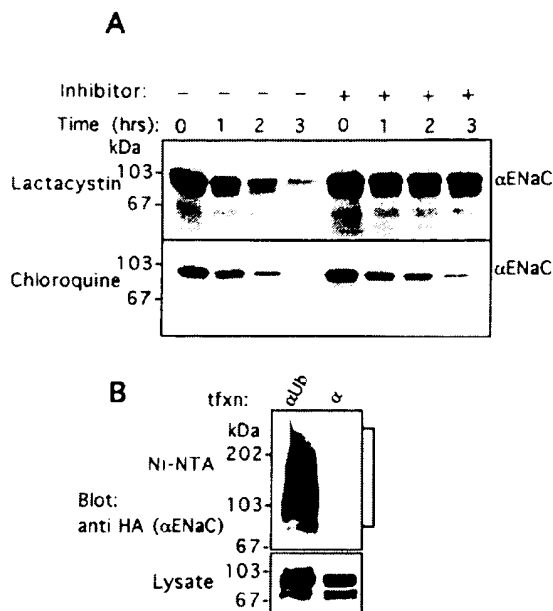


Fig. 8. The effect of inhibitors of the proteasome and late endosomes/lysosomes on the stability of total cellular pool of  $\alpha\beta\gamma$ ENaC.  $\alpha\beta\gamma$ ENaC expressed in MDCK cells were labelled with [ $^{35}$ S]Met and Cys for 2 h, and chased for the indicated times in the absence (–) or presence (+) of: (A) 10  $\mu$ M lactacystin added during the pulse and the chase periods, or (B) 0.4 mM chloroquine added during the chase period. The average increase in half-life for three to six independent experiments as represented in this figure are:  $\alpha$ ENaC: 2.7- and 2.1-fold increase for chloroquine and lactacystin inhibition respectively;  $\gamma$ ENaC: 1.3- and 1.7-fold increase for chloroquine and lactacystin. A similar pattern of inhibition of  $\alpha\beta\gamma$ ENaC degradation was observed with either lactacystin or chloroquine treatment of  $\alpha\beta\gamma$ ENaC expressed in NIH-3T3 cells (not shown).

lysosomal system in the case of several transmembrane proteins. In order to determine the mechanism(s) responsible for the rapid degradation (of total cellular pool) of ENaC seen in Figure 1, we tested the effect of inhibitors of either the proteasome or the endosomal/lysosomal system on the half-life of  $\alpha\beta\gamma$ ENaC expressed in MDCK cells using pulse-chase experiments. Our results show that when the potent proteasome inhibitor lactacystin (10  $\mu$ M; Fenteany *et al.*, 1995) was added during the 2 h pulse and the subsequent chase period, there was an attenuation of channel degradation (2.1- and 1.7-fold increase in half-life of  $\alpha$  and  $\gamma$ ENaC respectively; Figure 8A). This suggests an involvement of the proteasome in ENaC degradation. However, chloroquine (0.4 mM), a weak base that dissipates the late endosome/lysosome acidic pH thereby inhibiting proteolysis in these compartments, also led to a significant inhibition (2.7- and 1.3-fold increase in half-life of the  $\alpha$  and  $\gamma$  subunits respectively) of ENaC degradation when added during the chase period (Figure 8B). Our results, therefore, suggest that both the proteasomes and the endosomes/lysosomes are likely to play a role in the degradation of ENaC. One possible explanation for this dual mode of degradation may be that the individual ENaC subunits which are unassembled are targeted for proteasome degradation, whereas the properly assembled  $\alpha\beta\gamma$ ENaC subunits are subject to degradation by late endosomes/lysosomes. To test whether the unassembled subunits are indeed degraded by the proteasomes and not by the lysosomes, we used a MDCK



**Fig. 9.** Ubiquitination and mode of degradation of  $\alpha$ ENaC expressed alone in MDCK cells. **(A)** HA-tagged  $\alpha$ ENaC stably expressed in MDCK cells was labelled with  $^{35}$ S Met and Cys for 2 h, and chased for the indicated times in the absence (–) or presence (+) of 10  $\mu$ M lactacystin added during the pulse and the chase periods (upper panel), or 0.4 mM chloroquine added during the chase period (lower panel), as described in Figure 8 above. **(B)** Ubiquitination of  $\alpha$ ENaC transfected with His-Ub (Ub) into Hek-293 cells. Histidinated (ubiquitinated) proteins were precipitated on Ni-NTA agarose beads, proteins separated on 7% SDS-PAGE and immunoblotted with anti-HA antibodies, to detect ubiquitinated species of  $\alpha$ ENaC. The square bracket depicts ubiquitinated  $\alpha$ ENaC. The control ( $\alpha$ , right lane) was transfected with  $\alpha$ ENaC without His-Ub, and reveals no detectable ubiquitination, similar to cells transfected with  $\alpha$ ENaC alone.

cell line which expresses high levels of HA-tagged  $\alpha$ ENaC alone (Staub *et al.*, 1996). Despite high levels of expression, these cells display very little amiloride-sensitive  $\text{Na}^+$  currents when compared with MDCK cells expressing  $\alpha\beta\gamma$ ENaC together, as determined by whole cell patch clamp analysis (T. Ishikawa, Y. Marunaka and D. Rotin, unpublished). Moreover, expression of  $\alpha$ ENaC alone in *Xenopus* oocytes leads to a severely reduced ENaC activity due to a reduced number of channels at the cell surface (Canessa *et al.*, 1994a; Firsov *et al.*, 1996). We therefore tested whether  $\alpha$ ENaC expressed alone is ubiquitinated and whether it is degraded by proteasomes. Figure 9B shows that transfection of  $\alpha$ ENaC into Hek-293 cells together with the His-Ub construct led to a massive ubiquitination of this subunit. Moreover, pulse-chase experiments performed with  $\alpha$ ENaC stably expressed in MDCK cells reveal a strong inhibition of  $\alpha$ ENaC degradation by 10  $\mu$ M lactacystin (Figure 9A, upper panel), whereas chloroquine (0.4 mM) was largely ineffective (Figure 9A, lower panel). These results, therefore, demonstrate that expression of the  $\alpha$ ENaC subunit alone, which can not properly assemble into a channel in the absence of  $\beta\gamma$ ENaC, is targeted for proteasomal degradation.

## Discussion

The results presented here demonstrate collectively that ENaC stability and function are modulated by ubiquitination. Our current results show that ENaC is a short lived protein, with a half-life of  $\sim 1$  h for at least 2 of its subunits. This short  $t_{1/2}$  was detected in ENaC heterologously expressed in *Xenopus* oocytes, in ENaC transfected into either epithelial (MDCK) cells or fibroblast (NIH-3T3), or in xENaC endogenously expressed in A6 cells (B.C. Rossier, personal communication). The accumulation of ENaC following treatment of cells with the weak base chloroquine (or with  $\text{NH}_4\text{Cl}$ ; our unpublished data) which dissipate the acidic pH in late endosomes/lysosomes, suggests the involvement of the endosomal/lysosomal pathway in ENaC degradation. However, our findings that the half-life of the ENaC subunits is also prolonged when the cells are treated with lactacystin (or with MG132; data not shown), indicate that the proteasome is involved in ENaC breakdown as well. One possible explanation for these dichotomous data may be that a portion of the ENaC subunits which do not become properly assembled in the ER may be degraded in a proteasome-dependent manner, whereas the properly assembled  $\alpha\beta\gamma$ ENaC is targeted to the cell surface and is subsequently degraded by late endosomes/lysosomes. Although we cannot currently preclude the possibility of a sequential course of events whereby lysosomal degradation is followed by proteasomal degradation, we believe different pools (assembled versus unassembled) of ENaC are targeted to the different pathways. This is based on our results demonstrating lactacystin-sensitive and chloroquine-insensitive degradation of  $\alpha$ ENaC when expressed alone, but chloroquine-sensitivity when expressed together with  $\beta\gamma$ ENaC, as well as our preliminary results demonstrating a small additive stabilization of  $\alpha$ ENaC by lactacystin plus chloroquine relative to each inhibitor alone (O. Staub and D. Rotin, unpublished data). We believe our data represent the first documented case where the same ubiquitinated protein (e.g.  $\alpha$ ENaC) can be degraded by either the proteasome or the lysosome, depending on its assembly/disassembly status.

Although we propose a lysosomal-mediated degradation of  $\alpha\beta\gamma$ ENaC when properly assembled, we currently do not know how much of that pool of protein is actually located at the plasma membrane at any one time. We believe, however, that the ubiquitination of  $\alpha$ - and  $\gamma$ ENaC we observed represents, at least in part, ubiquitinated mature channel at the plasma membrane and not just of excess unassembled ENaC chains. This conclusion is based on our finding of a tight correlation between ubiquitination of ENaC and its number (and function) at the cell surface: mutations of a cluster of Lys residues in  $\gamma$ ENaC (or  $\alpha$ - plus  $\gamma$ ENaC) lead to both a reduction of ubiquitination and increased number of channels at the plasma membrane, with a concomitant elevated  $\text{Na}^+$  channel activity. Moreover, our Brefeldin A experiments suggest that a significant fraction of this increase in channel numbers in the ubiquitination-defective ENaC mutant results from increased retention (or recycling) of ENaC at the cell surface. Thus, although we do not currently know at what point(s) during processing and plasma membrane incorporation of ENaC it becomes



ubiquitinated, the consequences of such ubiquitination are clearly affecting channel stability at the cell surface.

The fact that the status of ENaC ubiquitination determines its stability at the plasma membrane is intriguing, because so far it is not known how ubiquitination signals for, or is involved in, degradation of transmembrane proteins. In this regard, the involvement of ubiquitination in regulating ENaC degradation at the cell surface is similar to that of other recently described transmembrane proteins. A notable example is the ubiquitination-dependent vacuolar degradation of the *Saccharomyces cerevisiae* permeases Fur4 and Gap1, which require the presence of intact Rsp5 (the yeast homologue of Nedd4) for this degradation (Hein *et al.*, 1995; Galan *et al.*, 1996). We have previously demonstrated direct binding of ENaC to the ubiquitin-protein ligase Nedd4, by association of the WW domains of Nedd4 with the PY motifs of the ENaC subunits (Staub *et al.*, 1996). We do not know yet whether Nedd4 participates in the ubiquitination of the ENaC subunits described in this report. We can speculate, however, that if it does, this may have implications for Liddle syndrome, an hereditary form of hypertension caused by deletions/mutations within the PY motifs of  $\beta$ - or  $\gamma$ ENaC (Shimkets *et al.*, 1994; Hansson *et al.*, 1995a,b; Tamura *et al.*, 1996). Such mutations lead to increased  $\text{Na}^+$  channel activity due to increased channel number and opening at the plasma membrane (Schild *et al.*, 1995, 1996; Snyder *et al.*, 1995; Firsov *et al.*, 1996). The same mutations also lead to an inhibition of binding to Nedd4-WW domains (Staub *et al.*, 1996). Thus, we can speculate that the increase in retention of ENaC at the plasma membrane associated with Liddle syndrome may involve reduced ubiquitination, possibly by reduced binding to Nedd4. Future experiments will address this possibility.

Regardless of the link to Liddle syndrome, the observation that ENaC is ubiquitinated in living cells, and that this ubiquitination is critical for the regulation of channel degradation or stability at the plasma membrane and hence to channel activity, is by itself important, as it provides the first demonstration of regulation of ion channel function by ubiquitination. Clearly, a tight regulation of ENaC is necessary for maintenance of salt and water homeostasis; impairment of such regulation has been linked to several diseases, including not only Liddle syndrome, but also PHA1 (Chang *et al.*, 1996; Strautnieks *et al.*, 1996), pulmonary oedema (Hummler *et al.*, 1996) and cystic fibrosis (Stutts *et al.*, 1995). It remains to be identified whether any subsets of genetically determined hypertensive patients (Liddle syndrome or otherwise) indeed have mutations in the conserved lysine residues at the N-termini of  $\alpha$ - or  $\gamma$ ENaC which serve as attachment sites for ubiquitin.

Our data suggest that  $\gamma$ ENaC is the important, if not the predominant subunit which is regulating ubiquitination-mediated degradation of the  $\text{Na}^+$  channel. Ubiquitination of  $\alpha$ ENaC, however, also plays a role in channel stability, which becomes significant only when the key lysine residues in  $\gamma$ ENaC (K6-13) are lost. We propose therefore that loss of the main ubiquitination target of ENaC ( $\gamma$ K6-13) allows the ubiquitination of  $\alpha$ ENaC to partially compensate for this loss; consequently, losing those N-terminal lysines in both  $\gamma$ - and  $\alpha$ ENaC greatly stabilizes the channel. Our measurements of turnover rate of

$\alpha\beta\gamma$ ENaC indicate that the  $t_{1/2}$  of  $\beta$ ENaC is somewhat longer than that of  $\alpha$ - and  $\gamma$ ENaC. We currently do not know whether such a difference in  $t_{1/2}$  is biologically meaningful. However, it is curious that  $\beta$ ENaC (when expressed together with  $\alpha\gamma$ ENaC) does not become ubiquitinated despite the presence of multiple conserved N-terminal lysine residues, and that mutation to arginines of these conserved lysines did not lead to channel hyperactivation. This suggests that the ubiquitination-mediated regulation of channel stability is not targeting the  $\beta$  subunit directly, but rather indirectly, via regulation of  $\gamma$ - and  $\alpha$ ENaC. Since ENaC is only efficiently exported to the plasma membrane in the presence of all three subunits (Canessa *et al.*, 1994a; McDonald *et al.*, 1995; Firsov *et al.*, 1996), targeting any subunit for degradation is sufficient to dismantle the channel and abrogate its activity. The reason for the observed partial inhibition of ENaC activity in some of the Lys to Arg mutants of  $\beta$ ENaC is not known, but we speculate such mutations may cause the formation of defective, less well functioning channels, perhaps similar to the recently described G37S mutation in the N-terminus of  $\beta$ ENaC which causes PHA1 due to reduced ENaC activity (Chang *et al.*, 1996).

In summary, the work presented here demonstrates a fundamental role for ubiquitination in the regulation of ENaC function, via regulation of channel stability at the plasma membrane. This could provide a previously undescribed mechanism to regulate function of ion channels at the cell surface.

## Materials and methods

### Plasmids and constructs

Rat  $\alpha\beta\gamma$ ENaC (rENaC, hereafter called ENaC) cDNA was used for all studies. Plasmids used for transient transfection into Hek-293 cells:  $\alpha$ ENaC was tagged with a triple haemagglutinin (HA) epitope (YPYDVPDY) at its carboxy terminal end just upstream of the stop codon and subcloned into a pCMV4 plasmid (Andersson *et al.*, 1989). The addition of the tag at that position did not interfere with  $\text{Na}^+$  channel function as assessed by patch clamp analysis (T. Ishikawa, Y. Marunaka and D. Rotin, unpublished). Similarly, a FLAG epitope (DYKDDDDK) was introduced just before the stop codon at the carboxy terminus of  $\gamma$ ENaC and subcloned into the pCEP4 plasmid (Invitrogen). Lysine to arginine mutants of  $\alpha$ -,  $\beta$ - and  $\gamma$ ENaC were generated by substituting specific lysine residues with arginines using the PCR based mutagenesis described by Nelson and Long (1989). These point mutants, mostly of conserved lysines and all located at the N-termini of the ENaC subunits, were designated as follows (see Figure 4): In  $\alpha$ ENaC: K47 and K50 ( $\alpha$ K47,50R), K108 ( $\alpha$ K108R), K47, K50 and K108 ( $\alpha$ K47,50,108R) and K23, 26, 32, 47 and 50 ( $\alpha$ K23-50R); In  $\beta$ ENaC: K4,5 and 9 ( $\beta$ K4,5,9R), and K16, 23, 39, 47, 48 and 49 ( $\beta$ K16-49R); in  $\gamma$ ENaC: K6, 8, 10, 12, 13 ( $\gamma$ K6-13R), K26R ( $\gamma$ K26R), and K6-13 plus K26R ( $\gamma$ K6-13+26R). With the exception of K23, 27 and 32 in  $\alpha$ ENaC, all the above mutated lysines are conserved between rat, human and *Xenopus* (Canessa *et al.*, 1994a; McDonald *et al.*, 1994; Puoti *et al.*, 1995). All the above lysine to arginine mutants were subcloned into pSD5 for expression into *Xenopus* oocytes (Canessa *et al.*, 1994a). For expression in Hek-293 cells,  $\alpha$ K23-50R was subcloned into pCMV4 and  $\gamma$ K6-13R into pCEP4.

### Transfections and cell lines

MDCK cells stably expressing rat  $\alpha$ -,  $\beta$ - and  $\gamma$ ENaC together, or expressing only HA-tagged  $\alpha$ ENaC, were previously generated (Stutts *et al.*, 1995; Staub *et al.*, 1996) by transfecting cells with  $\alpha$ ENaC in pLkneo (Hirt *et al.*, 1992) which contains a dexamethasone-inducible promoter, together with  $\beta$ - and  $\gamma$ ENaC cloned into a CMV-promoter based vector and expressed constitutively. MDCK previously transfected with  $\alpha$ - and  $\beta$ ENaC (kindly provided by Drs Canessa and Rossier) were stably transfected with pCEP4 encoding either FLAG-tagged wt- $\gamma$ ENaC

or  $\gamma$ K6-13R ENaC. Cells were maintained in DMEM + 10% fetal bovine serum (FBS) + G418 (0.3 mg/ml) + 10  $\mu$ M amiloride, to prevent cellular Na<sup>+</sup> overload (+ 0.1 mg/ml hygromycin for the FLAG-tagged  $\gamma$ ENaC-expressing cells). For transient transfections, Hek-293 cells were transfected using lipofectamine, according to manufacturer instructions (Life Sciences).

#### Pulse-chase experiments

For pulse chase experiments, MDCK cells stably expressing  $\alpha$ -,  $\beta$ - and  $\gamma$ ENaC, HA-tagged  $\alpha$ ENaC alone, or FLAG-tagged wt- $\gamma$  or  $\gamma$ K6-13R ENaC, stably co-expressed with wt- $\alpha$ ENaC, were grown to confluency in 6-well plates (Costar) and induced overnight in induction medium [DMEM 10% FBS 20  $\mu$ M amiloride containing 1  $\mu$ M dexamethasone and 2 mM Na<sup>+</sup> butyrate (MDCK expressing  $\alpha\beta$ ENaC), or 1  $\mu$ M dexamethasone (MDCK expressing HA-tagged  $\alpha$ ENaC)]. Cells were washed three times in depletion medium (Induction medium without FBS, cysteine and methionine) and labelled at 37°C (in 5% CO<sub>2</sub> in air) for 2 h in labelling medium [Depletion medium + 0.1 mCi/ml of <sup>35</sup>S-containing cell labelling mix (Promix, Amersham)]. Cells were then washed three times with ice-cold Induction medium containing 10 mM unlabelled methionine and cysteine, and then chased in the same medium for various periods of times at 37°C (in 5% CO<sub>2</sub> in air). Where indicated, lactacystin (10  $\mu$ M) was added to the pulse and chase solutions, and chloroquine (0.4 mM) was added to the wash and chase solution only. Cells were then washed three times with ice-cold phosphate buffer saline (PBS), and lysed in lysis buffer (50 mM HEPES, pH 7.5, 150 mM NaCl, 1.5 mM MgCl<sub>2</sub>, 1 mM EGTA, 1% Triton X-100, 10% glycerol, 1 mM PMSF, 10  $\mu$ g/ml leupeptin, 10  $\mu$ g/ml pepstatin A, 10  $\mu$ g/ml aprotinin). Insoluble material was removed by centrifugation and the soluble fraction denatured with 2% SDS and boiling for 5 min at 95°C. The samples were then diluted with 11 volumes of lysis buffer and immunoprecipitations performed by adding polyclonal sera directed against either the N-terminus of  $\alpha$ ENaC (Roth *et al.*, 1994), the C-terminus of  $\beta$ ENaC or the C-terminus of  $\gamma$ ENaC (Duc *et al.*, 1994). Immunocomplexes were collected with protein A-sepharose, separated on 7% SDS-PAGE and detected by autoradiography.

#### Detection of ENaC ubiquitination in vivo

Hek-293 cells were transiently co-transfected with a mixture of plasmids encoding HA-tagged  $\alpha$ ENaC, untagged  $\beta$ ENaC and FLAG-tagged  $\gamma$ ENaC together with a construct encoding His-tagged ubiquitin (His-Ub), which expresses eight His-tagged ubiquitin molecules from a CMV promoter (Treier *et al.*, 1994). Twenty-four hours after transfection, cells were lysed in lysis buffer (containing also 50  $\mu$ M N-acetyl-L-leucyl-L-leucyl-L-norleucinal, LLNL), insoluble material removed by centrifugation and the soluble fraction denatured in 2% SDS and boiling at 95°C for 5 min. Samples were then diluted with 11 volumes of lysis buffer, Ni<sup>2+</sup>-NTA agarose beads (Qiagen) added to the lysate, and the mixture incubated on a rotator for 4 h at 4°C. The beads containing the histidinated (and thus ubiquitinated) bound proteins were washed twice with HNTG (20 mM HEPES, pH 7.5, 300 mM NaCl, 0.1% Triton X-100, 10% glycerol, 40 mM imidazole) and three times with lysis buffer. Bound proteins were separated on 7% SDS-PAGE, transferred to nitrocellulose and immunoblotted with either anti-HA antibodies (Babco), anti-FLAG antibodies (Kodak), or anti- $\beta$ ENaC antibodies directed against amino acids 559–636 at the C-terminus (Duc *et al.*, 1994) followed by HRP-conjugated secondary antibody and chemiluminescence (ECL Amersham) or Supersignal ULTRA Pierce detection.

#### Expression and function of ENaC channels in *Xenopus* oocytes

Complementary RNA (cRNA) of each  $\alpha$ -,  $\beta$ - and  $\gamma$ ENaC subunit, or their indicated mutants, were synthesized *in vitro* and equal amounts of subunit cRNA (5 ng total) at saturating concentration for maximal expression were injected into stage V oocytes. ENaC activity at the cell surface resulting from ENaC expression was determined with the two-electrode voltage-clamp technique by measurement of the amiloride-sensitive inward Na<sup>+</sup> current ( $I_{Na}$ ) at 100 mV holding potential, as previously described (Schild *et al.*, 1995, 1996). Where indicated, Brefeldin A (BFA, 10  $\mu$ g/ml) was added to the oocyte bathing medium 18 h after cRNA injection, and  $I_{Na}$  measured as described above at 0, 2, 4, 6 and 8 h post BFA addition. A Patch clamp technique was used to record single channel currents in the cell-attached configuration with Li<sup>+</sup> ions as permeant cation on defolliculated oocytes, as described previously (Canessa *et al.*, 1994a; Schild *et al.*, 1997).

#### Surface labelling of ENaC in oocytes

For binding experiments, the lysine to arginine mutations at the N-terminus of  $\alpha$ - or  $\gamma$ ENaC ( $\alpha$ K47-50R;  $\gamma$ K6-13R) were introduced into  $\alpha$ - or  $\gamma$ ENaC cDNA (respectively) which already contained a FLAG epitope at the ectodomains, located ~30 residues downstream of the first transmembrane domain (Firsov *et al.*, 1996). The addition of the FLAG tag at that position has no effect on channel function (Firsov *et al.*, 1996). Surface expression of ENaC channels was determined by specific binding of [<sup>125</sup>I]M<sub>2</sub>IgG<sub>1</sub> (M<sub>2</sub>Ab) to oocytes expressing FLAG-tagged  $\alpha\beta$ ENaC, as described previously (Firsov *et al.*, 1996). The equilibrium dissociation constant of specific [<sup>125</sup>I]M<sub>2</sub>IgG<sub>1</sub> (M<sub>2</sub>Ab) binding was 3 nM. Accordingly, 12 nM M<sub>2</sub>Ab were added to a Modified Barth's Saline (MBS) solution supplemented with 5% calf serum incubating the oocytes. After 1 h incubation at 4°C, each oocyte was washed eight times with 1 ml MBS solution and transferred individually to a gamma counter. The same oocyte was then used to measure amiloride-sensitive Na<sup>+</sup> current. M<sub>2</sub>Ab non-specific binding was detected with oocytes injected with ENaC cRNAs encoding non-tagged subunits.

#### Acknowledgements

We would like to thank Drs C.M. Canessa and B.C. Rossier for MDCK cells expressing  $\alpha\beta$ ENaC and anti- $\beta$ - and  $\gamma$ ENaC antibodies, Dr D. Firsov for preparation of iodinated antibodies, Drs M.J. Stutts and R.C. Boucher for the ENaC-expressing NIH-3T3 cells, and Dr D. Bohmann for the His-tagged ubiquitin construct. This work was supported by the Canadian CF Foundation (to D.R.), by the Medical Research Council (MRC) of Canada and a MRC Group Grant in Lung Development (to D.R.), by a grant from the International Human Frontier Science Program (IHFS) (to L.S. and D.R.), and by a grant from the Swiss National Foundation for Scientific Research to L.S. (No. 31-39435.93). A.C. is supported by the Israeli Academy of Sciences, the German-Israeli Foundation for Research and Scientific Development (G.I.F.), the Council for Tobacco Research, Inc. (CTR), and the UK-Israel Binational Biotechnology Foundation. K.B. is supported by MINERVA and by HFSP Fellowships. O.S. was supported by a Fellowship from the Canadian CF Foundation, and D.R. was a recipient of a Scholarship from the MRC of Canada.

#### References

- Andersson, S., Davis, D.L., Dahlbaeck, H., Joernvall, H. and Russell, D.W. (1989) Cloning, structure, and expression of the mitochondrial cytochrome P-450 sterol 26-hydroxylase, a bile acid biosynthetic enzyme. *J. Biol. Chem.*, **264**, 8222–8229.
- Botero-Velez, M., Curtis, J.J. and Warnock, D.G. (1994) Brief report: Liddle's syndrome revisited. *New Engl. J. Med.*, **330**, 178–181.
- Brodsky, J.L. and McCracken, A.A. (1997) ER-associated and proteasome-mediated protein degradation: how two topologically restricted events came together. *Trends Cell Biol.*, **7**, 151–156.
- Canessa, C.M., Horisberger, J.-D. and Rossier, B.C. (1993) Epithelial sodium channel related to proteins involved in neurodegeneration. *Nature*, **361**, 467–470.
- Canessa, C.M., Schild, L., Buell, G., Thorens, B., Gautschi, I., Horisberger, J.-D. and Rossier, B.C. (1994a) Amiloride-sensitive epithelial Na<sup>+</sup> channel is made of three homologous subunits. *Nature*, **367**, 463–467.
- Canessa, C.M., Mériat, A.-M. and Rossier, B.C. (1994b) Membrane topology of the epithelial sodium channel in intact cells. *Am. J. Physiol.*, **267**, C1682–C1690.
- Cenciarelli, C., Hou, D., Hsu, K., Rellahan, B.L., Wiest, D.L., Smith, H.T., Fried, V.A. and Weissman, A.M. (1992) Activation-induced ubiquitination of the T cell antigen receptor. *Science*, **257**, 795–797.
- Chang, S.S. *et al.* (1996) Mutations in the subunits of the epithelial sodium channel cause salt wasting with hyperkalaemic acidosis, pseudohypoaldosteronism type I. *Nature Genet.*, **12**, 248–253.
- Ciechanover, A. (1994) The ubiquitin-proteasome proteolytic pathway. *Cell*, **79**, 13–21.
- Deshaies, R.J. (1995) Make it or break it: The role of ubiquitin-dependent proteolysis in cellular regulation. *Trends Cell Biol.*, **5**, 428–434.
- Duc, D., Farman, N., Canessa, C.M., Bonvalet, J.-P. and Rossier, B.C. (1994) Cell-specific expression of epithelial sodium channel  $\alpha$ ,  $\beta$  and  $\gamma$  subunits in aldosterone-responsive epithelia from the rat: localization by *in situ* hybridization and immunocytochemistry. *J. Cell Biol.*, **127**, 1907–1921.
- Egner, R. and Kuchler, K. (1996) The yeast multidrug transporter Pdr5 of the plasma membrane is ubiquitinated prior to endocytosis and degradation in the vacuole. *FEBS Lett.*, **378**, 177–181.

- Fenteany, G., Standaert, R.F., Lane, W.S., Choi, S., Corey, E.J. and Schreiber, S.L. (1995) Inhibition of proteasome activities and subunit-specific amino-terminal threonine modification by lactacystin. *Science*, **268**, 726–731.
- Firsov, D., Schild, L., Gautschi, I., Merrill, A.-M., Schneeberger, E. and Rossier, B.C. (1996) Cell surface expression of the epithelial Na<sup>+</sup> channel and a mutant causing Liddle syndrome: a quantitative approach. *Proc. Natl. Acad. Sci. USA*, **93**, 15370–15375.
- Galan, J.M., Moreau, V., André, B., Volland, C. and Haguenaer-Tsapis, R. (1996) Ubiquitination mediated by the Nplp Rsp5p ubiquitin-protein ligase is required for endocytosis of the yeast uracil permease. *J. Biol. Chem.*, **271**, 10946–10952.
- Gancheva-Garbova, Z., Theroux, S.J. and Davis, R.J. (1995) The epidermal growth factor receptor is covalently linked to ubiquitin. *Oncogene*, **11**, 2649–2655.
- Garty, H. and Palmer, L.G. (1997) Epithelial sodium channels: function, structure, and regulation. *Physiol. Rev.*, **77**, 359–396.
- Geering, K., Beggah, A., Good, P., Girardet, S., Roy, S., Schaer, D. and Jaumin, P. (1996) Oligomerization and maturation of Na,K-ATPase: Functional interaction of the cytoplasmic NH2 terminus of the beta subunit with the alpha subunit. *J. Cell Biol.*, **133**, 1193–1204.
- Hansson, J.H. et al. (1995a) Hypertension caused by a truncated epithelial sodium channel gamma subunit: Genetic heterogeneity of Liddle syndrome. *Nature Genet.*, **11**, 76–82.
- Hansson, J.H., Schild, L., Lu, Y., Wilson, T.A., Gautschi, I., Shimkets, R.A., Nelson-Williams, C., Rossier, B.C. and Lifton, R.P. (1995b) A de novo missense mutation of the beta subunit of the epithelial sodium channel causes hypertension and Liddle syndrome, identifying a proline-rich segment critical for regulation of channel activity. *Proc. Natl. Acad. Sci. USA*, **25**, 11495–11499.
- Hein, C., Springael, J.Y., Volland, C., Haguenaer-Tsapis, R. and André, B. (1995) NPII, an essential yeast gene involved in induced degradation of Gap1 and Fur4 permeases, encodes the Rsp5 ubiquitin-protein ligase. *Mol. Microbiol.*, **18**, 77–87.
- Hicke, L. and Riezman, H. (1996) Ubiquitination of a yeast plasma membrane receptor signals its ligand-stimulated endocytosis. *Cell*, **84**, 277–287.
- Hilt, W. and Wolf, D.H. (1996) Proteasomes: destruction as a programme. *Trends Biochem. Sci.*, **21**, 96–102.
- Hirt, R.P., Poulain-Godefroy, O., Billotte, J., Kraehenbuehl, J.-P. and Fasel, N. (1992) Highly inducible synthesis of heterologous proteins in epithelial cells carrying a glucocorticoid-responsive vector. *Gene*, **111**, 199–206.
- Hochstrasser, M. (1996) Protein degradation or regulation: Ub the judge. *Cell*, **84**, 813–815.
- Hummeler, E., Barker, P., Gatzky, J., Beermann, F., Verdumo, C., Schmidt, A., Boucher, R.C. and Rossier, B.C. (1996) Early death due to defective neonatal lung liquid clearance in alphaENaC-deficient mice. *Nature Genet.*, **12**, 325–328.
- Jensen, T.J., Loo, M.A., Pind, S., Williams, D.B., Goldberg, A.L. and Riordan, J.R. (1995) Multiple proteolytic systems including the proteasome, contribute to CFTR processing. *Cell*, **83**, 129–135.
- Jentsch, S. and Schlenker, S. (1995) Selective protein degradation: a journey's end within the proteasome. *Cell*, **82**, 881–884.
- Kölling, R. and Hollenberg, C.P. (1994) The ABC-transporter Ste6 accumulates in the plasma membrane in a ubiquitinated form in endocytosis mutants. *EMBO J.*, **13**, 3261–3271.
- Liddle, G.W., Bledsoe, T. and Coppage, W.S., Jr (1963) A familial renal disorder simulating primary aldosteronism but with negligible aldosterone secretion. *Trans. Assoc. Am. Physicians*, **76**, 199–213.
- Lingueglia, F., Voilley, N., Waldmann, R., Lazdunski, M. and Barbry, P. (1993) Expression cloning of an epithelial amiloride-sensitive Na<sup>+</sup> channel. A new channel type with homologies to *Caenorhabditis elegans* degenerins. *FEBS Lett.*, **318**, 95–99.
- Lingueglia, F., Renard, S., Waldmann, R., Voilley, N., Champigny, G., Plass, H., Lazdunski, M. and Barbry, P. (1994) Different homologous subunits of the amiloride-sensitive Na<sup>+</sup> channel are differently regulated by aldosterone. *J. Biol. Chem.*, **269**, 13736–13739.
- McDonald, F.J., Snyder, P.M., McCray, P.B., Jr and Welsh, M.J. (1994) Cloning, expression, and distribution of a human amiloride-sensitive Na<sup>+</sup> channel. *Am. J. Physiol.*, **266**, L728–L734.
- McDonald, F.J., Price, M.P., Snyder, P.M. and Welsh, M.J. (1995) Cloning and expression of the beta- and gamma-subunits of the human epithelial sodium channel. *Am. J. Physiol.*, **268**, C1157–C1163.
- Miyazawa, K., Toyama, K., Gotoh, A., Hendrie, P.C., Mantel, C. and Broxmeyer, H.E. (1994) Ligand-dependent polyubiquitination of c-kit gene product: a possible mechanism of receptor down modulation in M07e cells. *Blood*, **83**, 137–145.
- Mori, S., Heldin, C.-H. and Claesson-Welsh, L. (1992) Ligand-induced polyubiquitination of the platelet-derived growth factor beta-receptor. *J. Biol. Chem.*, **267**, 6429–6434.
- Nelson, R.M. and Long, G.L. (1989) A general method of site-specific mutagenesis using a modification of the *Thermus aquaticus* polymerase chain reaction. *Anal. Biochem.*, **180**, 147–151.
- O'Brodovich, H. (1995) The role of active Na<sup>+</sup> transport by lung epithelium in the clearance of airspace fluid. *New Horizons*, **3**, 240–247.
- Palombella, V., Rando, O., Goldberg, A.L. and Maniatis, T. (1994) Ubiquitin and the proteasome are required for processing the NF-kappaB1 precursor and the activation of NF-kappaB. *Cell*, **78**, 773–785.
- Paolini, R. and Kinet, J.-P. (1993) Cell surface control of the multibubiquitination and debubiquitination of high-affinity immunoglobulin E receptors. *EMBO J.*, **12**, 779–786.
- Puoti, A., May, A., Canessa, C.M., Horisberger, J.-D., Schild, L. and Rossier, B.C. (1995) The highly selective low-conductance epithelial Na<sup>+</sup> channel of *Xenopus laevis* A6 kidney cells. *Am. J. Physiol.*, **38**, C188–C197.
- Renard, S., Lingueglia, F., Voilley, N., Lazdunski, M. and Barbry, P. (1994) Biochemical analysis of the membrane topology of the amiloride-sensitive Na<sup>+</sup> channel. *J. Biol. Chem.*, **269**, 12981–12986.
- Rossier, B.C. and Palmer, L.G. (1992) Mechanisms of aldosterone action on sodium and potassium transport. In Seldin, D.W. and Giebisch, G. (eds), *The Kidney: Physiology and Pathophysiology*. Raven Press, New York, USA, pp. 1373–1409.
- Rotin, D., Bar-Sagi, D., O'Brodovich, H., Merilainen, J., Lehto, P.V., Canessa, C.M., Rossier, B.C. and Downey, G.P. (1994) A SH3 binding region in the epithelial Na<sup>+</sup> channel (ENaC) mediates its localization at the apical membrane. *EMBO J.*, **13**, 4440–4450.
- Saumon, G. and Basset, G. (1993) Electrolyte and fluid transport across the mature alveolar epithelium. *J. Appl. Physiol.*, **74**, 1–15.
- Scheffner, M., Huibregtse, J.M., Vierstra, R. and Howley, P.M. (1993) The HPV-16 E6 and E6-AP complex functions as a ubiquitin-protein ligase in the ubiquitination of p53. *Cell*, **75**, 495–505.
- Schild, L., Canessa, C.M., Shimkets, R.A., Warnock, D.G., Lifton, R.P. and Rossier, B.C. (1995) A mutation in the epithelial sodium channel causing Liddle's disease increases channel activity in the *Xenopus laevis* oocyte expression system. *Proc. Natl. Acad. Sci. USA*, **92**, 5699–5703.
- Schild, L., Lu, Y., Gautschi, I., Schneeberger, E., Lifton, R.P. and Rossier, B.C. (1996) Identification of a PY motif in the epithelial Na<sup>+</sup> channel subunits as a target sequence for mutations causing channel activation found in Liddle syndrome. *EMBO J.*, **15**, 2381–2387.
- Schild, L., Schneeberger, E., Gautschi, I. and Firsov, D. (1997) Identification of amino acid residues in the alpha, beta and gamma subunits of the epithelial sodium channel (ENaC) involved in amiloride block and ion permeation. *J. Gen. Physiol.*, **109**, 15–26.
- Shimkets, R.A. et al. (1994) Liddle's syndrome: heritable human hypertension caused by mutations in the beta subunit of the epithelial sodium channel. *Cell*, **79**, 407–414.
- Snyder, P.M., McDonald, F.J., Stokes, J.B. and Welsh, M.J. (1994) Membrane topology of the amiloride-sensitive epithelial sodium channel. *J. Biol. Chem.*, **269**, 24379–24383.
- Snyder, P.M., Price, M.P., McDonald, F.J., Adams, C.M., Volk, K.A., Zeiger, B.G., Stokes, J.B. and Welsh, M.J. (1995) Mechanism by which Liddle's syndrome mutations increase activity of a human epithelial Na<sup>+</sup> channel. *Cell*, **83**, 969–978.
- Staub, O., Dho, S., Henry, P.C., Correa, J., Ishikawa, T., McGlade, J. and Rotin, D. (1996) WW domains of Nedd4 bind to the proline-rich PY motifs in the epithelial Na<sup>+</sup> channel deleted in Liddle's syndrome. *EMBO J.*, **15**, 2371–2380.
- Strautnick, S.S., Thompson, R.J., Gardiner, R.M. and Chung, E. (1996) A novel splice-site mutation in the gamma subunit of the epithelial sodium channel gene in three pseudohypoaldosteronism type I families. *Nature Genet.*, **13**, 248–250.
- Strous, G.J., Van Kerkhof, P., Govers, R., Ciechanover, A. and Schwartz, A.L. (1996) The ubiquitin conjugation system is required for ligand-induced endocytosis and degradation of the growth hormone receptor. *EMBO J.*, **15**, 3806–3812.
- Stuts, M.J., Canessa, C.M., Olsen, J.C., Hamrick, M., Cohn, J.A., Rossier, B.C. and Boucher, R.C. (1995) CFTR as a cAMP-dependent regulator of sodium channels. *Science*, **269**, 847–850.

- Tamura,H., Schild,L., Enomoto,N., Matsui,N., Marumo,F., Rossier,B.C. and Sasaki,S. (1996) Liddle disease caused by a missense mutation of beta subunit of the epithelial sodium channel gene. *J. Clin. Invest.*, **97**, 1780-1784.
- Treier,M., Staszewski,L.M. and Bohmann,D. (1994) Ubiquitin-dependent c-Jun degradation *in vivo* is mediated by the  $\delta$  domain. *Cell*, **78**, 787-798.
- Voilley,N., Lingueglia,E., Champigny,G., Mattéi,M.-G., Waldmann,R., Lazdunski,M. and Barbry,P. (1994) The lung amiloride-sensitive Na<sup>+</sup> channel: Biophysical properties, pharmacology, ontogenesis, and molecular cloning. *Proc. Natl Acad. Sci. USA*, **91**, 247-251.
- Ward,C.L., Omura,S. and Kopito,R.R. (1995) Degradation of CFTR by the ubiquitin-proteasome pathway. *Cell*, **83**, 121-127.

*Received on April 23, 1997; revised on August 11, 1997*